Pol. J. Environ. Stud. Vol. XX, No. X (XXXX), 1-13
DOI: *10.15244/pjoes/202197* ONLINE PUBLICATION DATE: 2025-04-16

Original Research

Improved Recognition Method of Fuzzy Attribute Interval and Its Application in Risk Assessment of Debris Flow

Xingrong Liu[1], Ziqiang Zhou[1], Sheng Wang[2, 3, 4]*, Tao Wen[4], Xiaowei Wang[3], Ying Sai[4], Jian Tao[4]

[1]Geological Hazards Prevention Institute, Gansu Academy of Sciences, Lanzhou 730000, China
[2]State Key Laboratory of Mountain Bridge and Tunnel Engineering, Chongqing Jiaotong University, Chongqing 400074, China
[3]School of Civil Engineering, Chongqing Jiaotong University, Chongqing 400074, China
[4]School of Civil Engineering, Yangtze Normal University, Chongqing 408100, China

Received: 5 September 2024
Accepted: 22 February 2025

Abstract

Debris flow is one of the most frequent and harmful natural disasters globally. Risk assessment is a crucial approach for predicting the risk level and potential consequences associated with debris flow. This study aims to develop a method for the risk recognition of fuzzy attribute interval that provides a scientific basis for the early control and prevention of debris flow disasters. The main factors affecting the occurrence of debris flow disasters are analyzed, then the risk assessment indices of debris flow gully and their grading criteria are presented. Giving the complexity of geological conditions and the uncertainty of factor values, a triangular fuzzy number including the lower limit, the most probable number, and the upper limit is introduced to quantify each evaluation index. The corresponding nonlinearly single-index attribute measure functions, stochastic combination method of multi-index attribute measure based on the single-index measure interval, and risk recognition analysis method are reconstructed. Fuzzy theory and the analytic hierarchy process are employed to establish a weighting method for the debris flow evaluation index. This method is used to evaluate the risk of ten typical debris flow gullies in the Longnan region. The results indicate that the method is in perfect accordance with the practical situations. Therefore, the recognition method of fuzzy attribute interval risk has better applicability, higher accuracy, and clearer risk grading discrimination, which has good prospects for further risk assessment of debris flow gullies.

Keywords: debris flow, risk assessment, evaluation index system, attribute interval recognition model, triangular fuzzy number

*e-mail: wshsdu@163.com

Introduction

Debris flows are a special kind of torrent generated by liquid-phase water runoff, such as meltwater from glaciers and snow, entrained with a large number of solid-phase granular materials such as clay and boulders [1-4]. It often occurs in gullies or slopes with strong terrain incision. Currently, debris flow is one of the most harmful natural disasters with the largest threatened population in the world, which has caused serious human casualties and economic losses [5, 6]. Under the influence of global climate change, the frequency, intensity, duration, and influencing scope of various extreme climate events (such as heavy rainfall) are becoming increasingly severe. Coupled with frequent tectonic movements and human activities, debris flow disasters are showing an increasing trend [7-9]. Therefore, it is of great practical significance to research the risk recognition and spatial distribution law of debris flow for early prevention and control of debris flows.

At present, several methods have been developed for risk assessment of debris flows [10-13], which can mainly be summarized into three categories. The first category is the numerical simulation analysis method, commonly including FLO-2D [14, 15], Debris-2D [16, 17], PFC [18], and SPH [19, 20]. PFC and SPH are mainly used to study the initiation mechanism and motion characteristics of debris flow, while FLO-2D and Debris-2D are widely used in risk assessment and zoning of debris flow. Wang et al. accurately reconstructed the dynamics of debris flow during typhoons through comprehensive numerical calculations combining the hydrologic model (SCS-CN) with the FLO-2D model, and then predicted the vulnerability and risk values of buildings by considering factors such as debris flow intensity, building vulnerability, and building economic value [21]. Nocentini et al. carried out a dynamic model by using two dynamic codes, DAN-W and FLO-2D, to evaluate the potential debris flow hazard [22]. Cao et al. used the FLO-2D to simulate the flow situation of the main river before rainfall, assess the debris flow risk under different rainfall frequencies, identify the high-risk debris flow gully in the basin, and delimit the high-risk residential area [23]. Zhang et al. used the Rapid Mass Motion Simulation (RAMMS) to quantitatively predict the hazard of debris flows with different recurrence periods (30, 50, and 100 years) and conducted a vulnerability assessment of the Xigou debris flows in the Three Gorges Reservoir area [24]. Ding et al. conducted a scientific assessment of the risk probability of three debris flows in Yunlong County through field geological surveys and using the FLO-2D professional simulation system [25]. The second category is the mathematical models of risk assessment, such as the analytic hierarchy process (AHP) [26], fuzzy comprehensive evaluation method [27, 28], grey correlation model [29, 30], ideal point method [31, 32], neural network [33], cloud model [34]. The third category is the risk zoning of geographic information systems. Xiao et al. proposed a method for zoning the potential sudden hazards of debris flows based on deep neural networks and analyzed the risk degree of potential sudden debris flow in each region [35]. Choi et al. developed a framework for risk assessment of regional debris flow, which was applied to Chuncheon City in South Korea [36]. Zhou et al. established a risk assessment model and a vulnerability assessment model based on the extra tree model and constructed a risk assessment of a debris flow model using the contributing weight superposition method [9]. Cui and Zou established risk assessment and mapping methods based on the dynamic process of debris flows and flash floods, as well as vulnerability assessment of risk factors [11]. In addition, Chen et al. Constructed three risk management contribution models using GIS and entropy-weighted grey correlation analysis methods [13]. Chen et al. proposed a method combining a probability-based model with numerical simulations to quantify the expected and direct economic losses caused by debris flows to buildings under various rainfall intensity scenarios [37]. Li et al. constructed a road risk assessment of debris flow model that includes an improved key indicator screening and weight assigning method to assess the debris flow risk under future climate change [38]. Sun et al. proposed a comprehensive risk assessment framework of regional debris flow, which consists of three main procedures: debris flow risk analyses based on the weight-of-evidence method, physical vulnerability analyses based on 12 indices, and risk calculation considering the natural attributes of debris flow and social attributes of linear engineering [39]. Although these methods have made progress in the risk analysis of debris flow, there are some shortcomings and restricted application conditions. The numerical simulation method can obtain some information about the debris flow disaster, such as flow velocity, flow rate, and mud depth, but the mechanical parameters of the rock-soil mass are difficult to obtain, and the numerical modeling and mechanical model are simplified. It is difficult to determine the values of the evaluation index in mathematical models, and each model has its own application restrictions. For example, the AHP and fuzzy evaluation models are highly subjective, and their results are easily affected by the knowledge level or experience of experts. The grey theory and neural network need a large number of prior samples. The geographic information system is mainly used to assess the risk level in a certain area rather than a single unit, which has the disadvantages of poor accuracy and difficulty in preventing and controlling debris flows.

In the present study, a new method to evaluate the risk of debris flow gully is proposed based on attribute measure theory. 8 important factors are selected to construct the risk assessment index system, and the risk grading criteria of evaluation indices are established. The value of the evaluation index is quantified as a small range of the triangular fuzzy interval number, rather than a fixed value. The attribute measure functions and risk recognition analysis method

are improved. The fuzzy theory-AHP weighting method is developed to determine the weight of the evaluation index. This method is applied to assess the risk of ten typical debris flow gullies in the Longnan region, analyze the risk levels of debris flow gullies, and compare the results calculated by the grey correlation model with the actual situations. This method can improve the accuracy of risk assessment results and provide a practical tool to assess the risk of debris flow gullies.

Material and Methods

Evaluation Index System of Debris Flow Risk

Selection of Risk Assessment Index

Whether the constructed evaluation index system is reasonable will directly affect the accuracy of risk assessment of debris flow. There are many factors affecting the risk of debris flow. If too many factors are considered, the assessment process will be complicated.

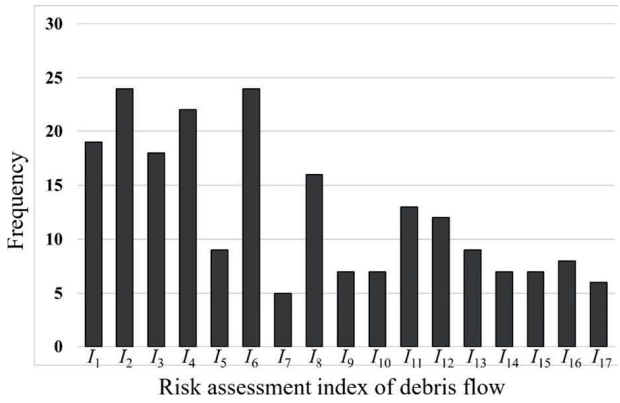

Fig. 1. The usage frequency statistics of risk assessment factors of debris flow.

Therefore, it is necessary to select important factors to construct the evaluation index system of debris flow. For this reason, we have carried out a large number of case statistical analyses and field investigations in the Longnan region [10, 27-29]. The main influencing factors and occurrence frequency of debris flow disaster are obtained, as shown in Fig. 1. In Fig. 1, I_1 is the maximum run-out volume at one time, I_2 is the watershed area, I_3 is the watershed incision density, I_4 is the main gully length, I_5 is the occurrence frequency of debris flow, I_6 is the maximum relative height difference of the watershed, I_7 is the proportion of unstable gully bed, I_8 is the maximum daily rainfall, I_9 is the bending coefficient of main gully, I_{10} is the vegetation coverage rate, I_{11} is the loose solid mass reserves, I_{12} is the longitudinal slope drop of the main gully, I_{13} is the ratio of length of sediment recharge section, I_{14} is the population density of the watershed, I_{15} is the slope degree, I_{16} is the stratum lithology, I_{17} is the distance from fault.

Based on the statistical results in Fig. 1, combined with the field investigation of debris flow gullies in the Longnan region, the maximum run-out volume at one time I_1, watershed area I_2, watershed incision density I_3, main gully length I_4, maximum relative height difference of the watershed I_6, maximum daily rainfall I_8, loose solid mass reserves I_{11}, and longitudinal slope drop of the main gully I_{12} are selected to establish the risk assessment index system of debris flow gully, as shown in Fig. 2.

Grade Criteria for Risk Assessment Index

According to the grading criteria of geological hazards, the risk levels of debris flow are classified as slight risk (I), medium risk (II), high risk (III), and extreme risk (IV). The risk level ranges from I to IV. The higher the risk level, the more serious the debris flow risk of the assessment object. On the basis

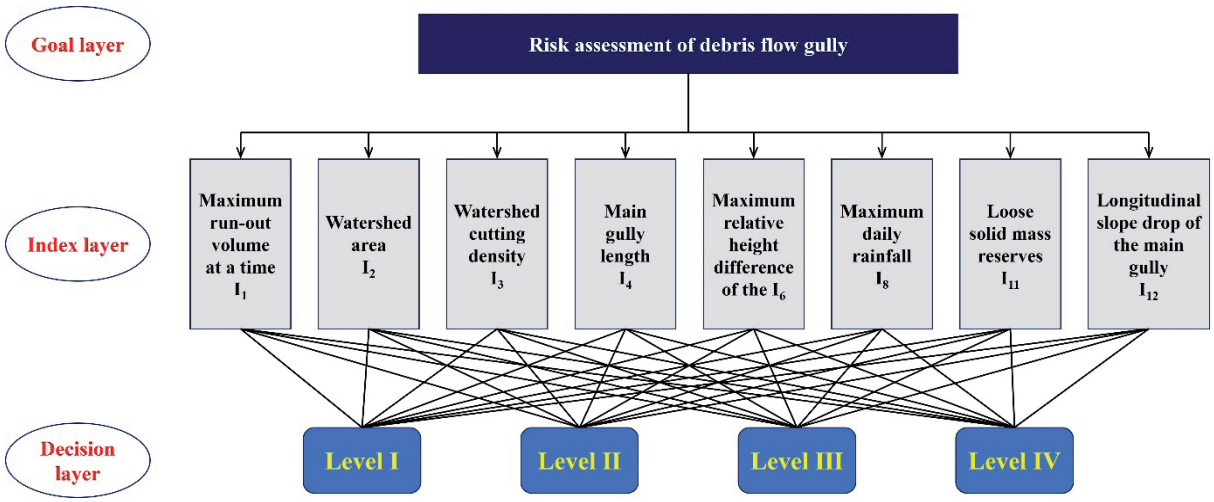

Fig. 2. Framework structure for risk assessment of debris flow gully.

Table 1. Grade criteria for risk assessment indices indexes of debris flow.

Evaluation index	I (Slight risk)	II (Medium risk)	III (high risk)	IV (Extreme risk)
Maximum run-out volume at one time I_1 (10^4 m^3)	≤0.5	0.5~1	1~10	≥10
Watershed area I_2 (km^2)	<0.5	0.5~10	10~35	≥35
Watershed incision density I_3 ($km \cdot km^{-2}$)	<5	5~10	10~20	≥20
Main gully length I_4 (km)	<1	1~5	5~10	≥10
Maximum relative height difference of the watershed I_6 (km)	≤0.2	0.2~0.5	0.5~1. 0	>1.0
Maximum daily rainfall I_8 (mm)	≤25	25~50	50~100	≥100
Loose substance reserves I_{11} (10^4 m^3)	≤10	10~100	100~200	≥200
Longitudinal slope drop of the main gully I_{12} (%)	≤5	5~15	15~30	≥30

of summarizing the existing achievements, the grade criteria for the risk assessment index of debris flow is proposed [10, 27-29], as shown in Table 1.

Improved Attribute Interval Recognition Model

The improved attribute interval recognition model is enhanced from three aspects: (1) Considering the fuzziness of the assignment information of the evaluation index, the triangular fuzzy interval number $[t_j^L, t_j^M, t_j^U]$ is used to assign the value of the evaluation index I_j instead of a fixed value. t_j^L, t_j^M, and t_j^U represent the lower limit, the most probable number, and the upper limit of the measure value of the index I_j, respectively. (2) Aiming at the complex nonlinear relationship between the value size of the evaluation index and the membership degree of risk level, the sine function is introduced to improve the traditional single-index attribute measure functions. (3) A combination weighting method is established based on AHP and triangular fuzzy theory.

Improved Attribute Mathematical Theory

The traditional attribute synthetic assessment theory can be divided into three parts: single-index attribute measure analysis, multi-index synthetic attribute measure analysis, and attribute recognition analysis.

Let $X = \{x_1, x_2, \ldots, x_n\}$ be the evaluation object space. Any assessment object x_i has m evaluation index I_j (j = 1, 2, …, m), and its measure value is expressed by t_j, where I_j represents the jth evaluation index. Each evaluation index I_j (j = 1, 2,…, m) is divided into K continuous risk level C_k (k = 1, 2,…, K). The support probability that the measure value t_j of I_j has the attribute of risk level C_k is expressed by the single-index attribute measure function μ_{ijk}. The probability that the assessment object x_i has the attribute of risk level C_k is expressed by the synthetic attribute measure function μ_{ik}.

(1) Single-index attribute measure analysis

First of all, the classification standard of the evaluation index I_j is defined, as shown in Table 2. When a_{jk} satisfies $a_{j0}<a_{j1}<\ldots<a_{jK}$ or $a_{i0}>a_{i1}>\ldots>a_{iK}$, let:

$$b_{jk} = \frac{a_{jk-1} + a_{jk}}{2} \tag{1}$$

Where a_{jk-1} and a_{jk} are the lower limit and the upper limit of the evaluation index I_j (j = 1, 2,…, m) belonging to risk level C_k (k = 1, 2, …, K), respectively.

$$d_{jk} = \min\left\{\left|b_{jk} - a_{jk}\right|, \left|b_{jk+1} - a_{jk}\right|\right\} \tag{2}$$

Where k = 1, 2, …, K-1.

When $a_{j0}<a_{j1}<\ldots<a_{jK}$ or $a_{i0}>a_{i1}>\ldots>a_{iK}$, the single-index attribute measure function is defined, and its expression is shown in Fig. 3. It can be seen from Fig. 3 that the single-index attribute measure value μ_{ijk} is linearly related to the measure value t_j of the evaluation index I_j. That is, the single-index attribute measure function is linear. The debris flow is a nonlinear complex dynamical system with multi-factors and multi-phase coupling, namely, the relationship between the attribute measure value and the measure value of the evaluation index is nonlinear. When the measure value t_j is small or big, its attribute measure value changes slowly. When the measure value is at a certain level, its attribute measure value changes rapidly. Therefore, the triangular fuzzy theory is introduced to nonlinearly improve the single-index attribute measure function.

When $a_{j0}<a_{j1}<\ldots<a_{jK}$, the single-index attribute measure function $\mu_{ijk}(t_j)$ is as follows:

Table 2. Classification standard of single evaluation index.

Evaluation index I_j	Risk level			
	C_1	C_2	…	C_K
I_1	a_{10}~a_{11}	a_{11}~a_{12}	…	a_{1K-1}~a_{1K}
I_2	a_{20}~a_{21}	a_{21}~a_{22}	…	a_{2K-1}~a_{2K}
…	…	…	…	…
I_m	a_{m0}~a_{m1}	a_{m1}~a_{m2}	…	a_{mK-1}~a_{mK}

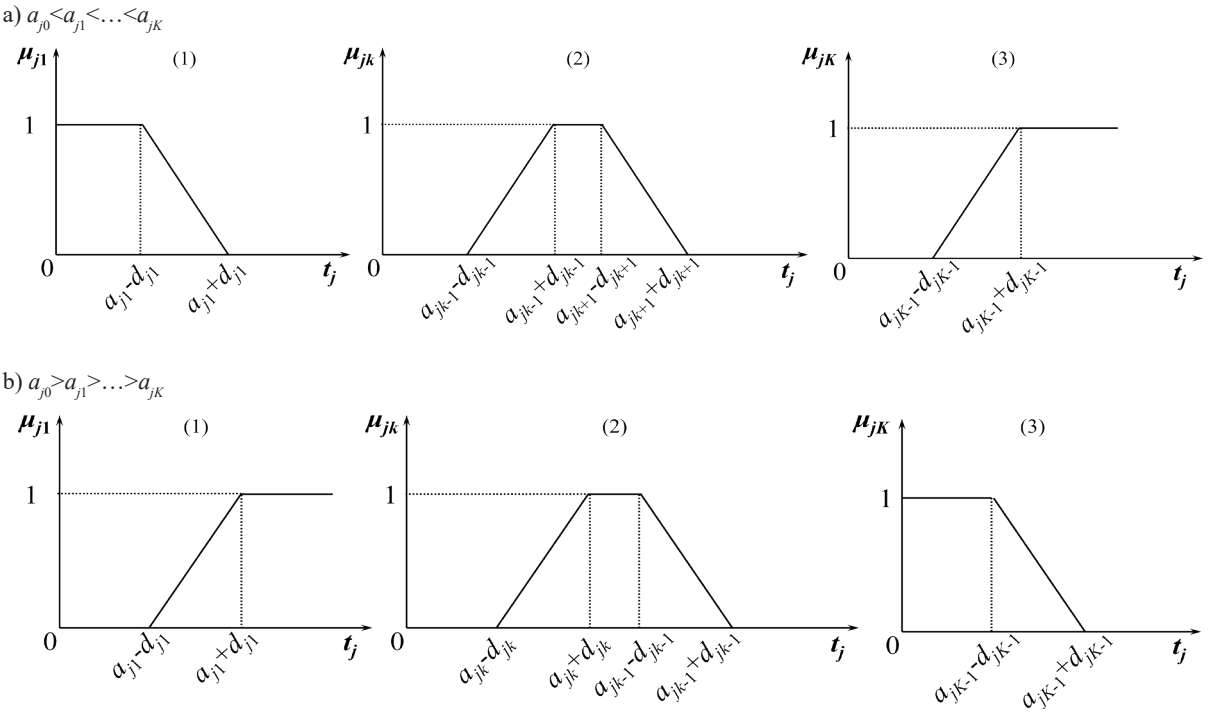

Fig. 3. Traditional single-index attribute measure function.

$$\mu_{ij1}(t_j)=\begin{cases}1 & t_j<a_{j1}-d_{j1}\\ \frac{1}{2}\sin\left(\frac{3}{2}\pi-\frac{a_{j1}+d_{j1}-t_j}{2d_{j1}}\pi\right)+\frac{1}{2} & a_{j1}-d_{j1}\le t_j\le a_{j1}+d_{j1}\\ 0 & t_j>a_{j1}+d_{j1}\end{cases} \tag{3}$$

$$\mu_{ijk}(t_j)=\begin{cases}0 & t_j<a_{jk-1}-d_{jk-1}\\ \frac{1}{2}\sin\left(\frac{3}{2}\pi-\frac{t_j-a_{jk-1}+d_{jk-1}}{2d_{jk-1}}\pi\right)+\frac{1}{2} & a_{jk-1}-d_{jk-1}\le t_j\le a_{jk-1}+d_{jk-1}\\ 1 & a_{jk-1}+d_{jk-1}<t_j<a_{jk}-d_{jk}\\ \frac{1}{2}\sin\left(\frac{3}{2}\pi-\frac{a_{jk}+d_{jk}-t_j}{2d_{jk}}\pi\right)+\frac{1}{2} & a_{jk}-d_{jk}\le t_j\le a_{jk}+d_{jk}\\ 0 & t_j>a_{jk}+d_{jk}\end{cases} \tag{4}$$

$$\mu_{ijK}(t_j)=\begin{cases}0 & t_j<a_{jK-1}-d_{jK-1}\\ \frac{1}{2}\sin\left(\frac{3}{2}\pi-\frac{t_j-a_{jK-1}+d_{jK-1}}{2d_{jK-1}}\pi\right)+\frac{1}{2} & a_{jK-1}-d_{jK-1}\le t_j\le a_{jK-1}+d_{jK-1}\\ 1 & t_j>a_{jK-1}+d_{jK-1}\end{cases} \tag{5}$$

When $a_{j0}<a_{j1}<\ldots<a_{jK}$, the single-index attribute measure function $\mu_{ijk}(t_j)$ is as follows:

$$\mu_{ij1}(t_j)=\begin{cases}0 & t_j<a_{j1}-d_{j1}\\ \frac{1}{2}\sin\left(\frac{3}{2}\pi-\frac{t_j-a_{j1}+d_{j1}}{2d_{j1}}\pi\right)+\frac{1}{2} & a_{j1}-d_{j1}\le t_j\le a_{j1}+d_{j1}\\ 1 & t_j>a_{j1}+d_{j1}\end{cases} \tag{6}$$

$$\mu_{ijk}(t_j)=\begin{cases}0 & t_j<a_{jk}-d_{jk}\\ \frac{1}{2}\sin\left(\frac{3}{2}\pi-\frac{t_j-a_{jk}+d_{jk}}{2d_{jk}}\pi\right)+\frac{1}{2} & a_{jk}-d_{jk}\le t_j\le a_{jk}+d_{jk}\\ 1 & a_{jk}+d_{jk}<t_j<a_{jk-1}-d_{jk-1}\\ \frac{1}{2}\sin\left(\frac{3}{2}\pi-\frac{a_{jk-1}+d_{jk-1}-t_j}{2d_{jk-1}}\pi\right)+\frac{1}{2} & a_{jk-1}-d_{jk-1}\le t_j\le a_{jk-1}+d_{jk-1}\\ 0 & t_j>a_{jk-1}+d_{jk-1}\end{cases} \tag{7}$$

$$\mu_{ijK}(t_j)=\begin{cases}1 & t_j<a_{jK-1}-d_{jK-1}\\ \frac{1}{2}\sin\left(\frac{3}{2}\pi-\frac{a_{jK-1}+d_{jK-1}-t_j}{2d_{jK-1}}\pi\right)+\frac{1}{2} & a_{jK-1}-d_{jK-1}\le t_j\le a_{jK-1}+d_{jK-1}\\ 0 & t_j>a_{jK-1}+d_{jK-1}\end{cases} \tag{8}$$

Where $j = 1, 2, \ldots, m$; $k = 1, 2, \ldots, K$.

Considering the complexity of the hazard-pregnant environment and the uncertainty of the values of the evaluation index, a small range interval $[t_j^L, t_j^M, t_j^U]$ is used to quantify the measure value t_j of the evaluation index I_j, which t_j^L, t_j^M, and t_j^U represent the lower limit, the most probable number, and the upper limit of the measure value of the index I_j, respectively.

The measured lower limit t_j^L, the most probable number t_j^M, and upper limit t_j^U are substituted into Eq. (3)~Eq. (8). Three single-index attribute measure vectors can be obtained. Their expressions are defined as follows:

$$\begin{cases} \mu_j^L = \left(\mu_{j1}^L, \mu_{j2}^L, \cdots, \mu_{jK}^L\right) \\ \mu_j^M = \left(\mu_{j1}^M, \mu_{j2}^M \cdots, \mu_{jK}^M\right) \\ \mu_j^U = \left(\mu_{j1}^U, \mu_{j2}^U, \cdots, \mu_{jK}^U\right) \end{cases} \tag{9}$$

(2) Multi-index synthetic attribute measure analysis

Since each evaluation index has three single-index attribute measure values μ_j^L, μ_j^M, and μ_j^U. The multi-index synthetic attribute measure has 3^m combinations. The calculation formula of the multi-index synthetic attribute measure value is as follows:

$$\mu_k = \sum_{j=1}^{m} \left(\omega_j \mu_{jk}\right) \tag{10}$$

Where w_j is the weight of the index I_j, which satisfies $0 \le w_j \le 1$, and $\sum_{i=1}^{n} w_i = 1$.

(3) Attribute recognition analysis

The confidence criterion is introduced to identify the risk level of the assessment object, and the confidence degree λ is between 0.6 and 0.7. Assuming that the risk level C_k are arranged in order, the risk level of the object to be evaluated is determined as follows:

When $C_1 < C_2 < \ldots < C_K$, if Eq.(11) is satisfied, the risk level of the assessment object is C_{k0}.

$$k_0 = \max\left\{k : \sum_{l=k}^{K} u_{xl} \ge \lambda, 1 \le k \le K\right\} \tag{11}$$

When $C_1 > C_2 > \ldots > C_K$, if Eq.(12) is satisfied, the risk level of the assessment object is C_{k0}.

$$k_0 = \min\left\{k : \sum_{l=1}^{k} u_{xl} \ge \lambda, 1 \le k \le K\right\} \tag{12}$$

Aiming at the improved attribute interval risk recognition method, two calculation methods of risk level recognition are proposed based on the traditional attribute recognition analysis.

a) Probability analysis method

Firstly, the synthetic attribute measure vector of each combination is obtained by using Eq. (10). Then, the risk level can be determined based on the confidence criteria. Each synthetic attribute measure vector corresponds to a risk level C_{k0}, and a total of 3^m C_{k0} can be obtained. Finally, the number of risk levels C_k (k=1, 2,…, K) is counted, and its proportion is calculated. The proportion of the most probable risk level is the largest.

b) Weighted average method

This method performs the weighted average on μ_{jk}^L, μ_{jk}^M, and μ_{jk}^U, to obtain the synthetic attribute measure vector. Then, the most probable risk level can be determined based on the attribute measure analysis. The calculation formula of the weighted average is as follows:

$$\mu_{jk} = \frac{\alpha\mu_{jk}^L + \beta\mu_{jk}^M + \gamma\mu_{jk}^U}{3} \tag{13}$$

In Eq. (13), α, β, and γ are the distribution coefficients of μ_{jk}^L, μ_{jk}^M, and μ_{jk}^U respectively, which can satisfy $\alpha + \beta + \gamma = 1$, $\beta > \alpha > 0$, and $\beta > \gamma > 0$. Their specific values can be determined by experts according to the actual situation.

According to the grade criteria in Table 2, the ingle-index attribute functions for risk assessment of debris flow are constructed, as shown in Table 3.

Triangular Fuzzy Theory-Analytic Hierarchy Process

The weights of the evaluation index have a direct impact on the accuracy and rationality of the assessment results, which are crucial to the risk level of the assessment object. To give full play to the subjective initiative of experts and the fuzziness and uncertainty of the influencing factors, the triangular fuzzy theory (TFT) is introduced to improve the analytic hierarchy process (AHP), and a new weighting method is established to determine the weight of the evaluation index.

A triangular fuzzy number $R_{ij} = (r^l_{ij}, r^m_{ij}, r^u_{ij})$ is used to quantify the relative importance between the index I_i (i = 1, 2, …, m) and the index I_j (j = 1, 2, …, m), where r^l, r^m, and r^u represent the lower limit, intermediate value, and upper limit of the relative importance between the indices, respectively. The values of these numbers are determined according to the 1~9 scale method as shown in Table 4.

An n-order judgment matrix can be formed from R_{ij}(i, j = 1, ..., n), namely $R = (R_{ij})_{n\times n}$. To test the consistency of the judgment matrix R, the triangular fuzzy opinions should be aggregated first.

$$m_{ij} = \frac{r_{ij}^L + 2r_{ij}^M + r_{ij}^U}{4} \quad (i, j = 1, 2, \cdots, n) \tag{14}$$

$$M = (m_{ij})_{n\times n} \tag{15}$$

The weights of each evaluation index can be calculated based on the judgment matrix M.

Table 3. single-index attribute measure functions of debris flow assessment.

Function	I	II	III	IV
I_1	$\mu_{11}(t_1)=\begin{cases}1 & t_1<0.25\\ \frac{1}{2}\sin(2t_1\pi)+\frac{1}{2} & 0.25\le t_1\le 0.75\\ 0 & t_1>0.75\end{cases}$	$\mu_{12}(t_1)=\begin{cases}0 & t_1<0.25\\ \frac{1}{2}\sin(2\pi-2t_1\pi)+\frac{1}{2} & 0.25\le t_1\le 0.75\\ \frac{1}{2}\sin(2t_1-1)\pi+\frac{1}{2} & 0.75\le t_1\le 1.25\\ 0 & t_1>1.25\end{cases}$	$\mu_{13}(t_1)=\begin{cases}0 & t_1<0.75\\ \frac{1}{2}\sin(3\pi-2t_1\pi)+\frac{1}{2} & 0.75\le t_1\le 1.25\\ 1 & 1.25\le t_1\le 5.5\\ \frac{1}{2}\sin\left(\frac{3}{2}\pi-\frac{14.5-t_1}{9}\pi\right)+\frac{1}{2} & 5.5\le t_1\le 14.5\\ 0 & t_1>14.5\end{cases}$	$\mu_{14}(t_1)=\begin{cases}0 & t_1<5.5\\ \frac{1}{2}\sin\left(\frac{3}{2}\pi-\frac{t_1-5.5}{9}\pi\right)+\frac{1}{2} & 5.5\le t_1\le 14.5\\ 1 & t_1>14.5\end{cases}$
I_2	$\mu_{21}(t_2)=\begin{cases}1 & t_2<0.25\\ \frac{1}{2}\sin(2t_2\pi)+\frac{1}{2} & 0.25\le t_2\le 0.75\\ 0 & t_2>0.75\end{cases}$	$\mu_{22}(t_2)=\begin{cases}0 & t_2<0.25\\ \frac{1}{2}\sin(2\pi-2t_2\pi)+\frac{1}{2} & 0.25\le t_2\le 0.75\\ 1 & 0.75<t_2<5.25\\ \frac{1}{2}\sin\left(\frac{3}{2}\pi-\frac{14.75-t_2}{9.5}\pi\right)+\frac{1}{2} & 5.25\le t_2\le 14.75\\ 0 & t_2>14.75\end{cases}$	$\mu_{23}(t_2)=\begin{cases}0 & t_2<5.25\\ \frac{1}{2}\sin\left(\frac{3}{2}\pi-\frac{t_2-5.25}{9.5}\pi\right)+\frac{1}{2} & 5.25\le t_j\le 14.75\\ 1 & 14.75<t_j<27.5\\ \frac{1}{2}\sin\left(\frac{3}{2}\pi-\frac{42.5-t_j}{15}\pi\right)+\frac{1}{2} & 27.5\le t_j\le 42.5\\ 0 & t_j>42.5\end{cases}$	$\mu_{24}(t_2)=\begin{cases}0 & t_2<27.5\\ \frac{1}{2}\sin\left(\frac{3}{2}\pi-\frac{t_2-27.5}{15}\pi\right)+\frac{1}{2} & 27.5\le t_2\le 42.5\\ 1 & t_2>42.5\end{cases}$
I_3	$\mu_{31}(t_3)=\begin{cases}1 & t_3<5\\ \frac{1}{2}\sin\left(\frac{t_3}{10}\pi\right)+\frac{1}{2} & 5\le t_3\le 15\\ 0 & t_3>15\end{cases}$	$\mu_{32}(t_3)=\begin{cases}0 & t_3<5\\ \frac{1}{2}\sin\left(2\pi-\frac{t_3}{10}\pi\right)+\frac{1}{2} & 5\le t_3\le 15\\ 1 & 15<t_3<55\\ \frac{1}{2}\sin\left(\frac{3}{2}\pi-\frac{145-t_3}{90}\pi\right)+\frac{1}{2} & 55\le t_3\le 145\\ 0 & t_3>145\end{cases}$	$\mu_{33}(t_3)=\begin{cases}0 & t_3<55\\ \frac{1}{2}\sin\left(\frac{3}{2}\pi-\frac{t_3-55}{90}\pi\right)+\frac{1}{2} & 55\le t_3\le 145\\ 1 & 145<t_3<150\\ \frac{1}{2}\sin\left(\frac{t_3}{100}\pi-\pi\right)+\frac{1}{2} & 150\le t_3\le 250\\ 0 & t_3>250\end{cases}$	$\mu_{34}(t_3)=\begin{cases}0 & t_3<150\\ \frac{1}{2}\sin\left(3\pi-\frac{t_3}{100}\pi\right)+\frac{1}{2} & 150\le t_3\le 250\\ 1 & t_3>250\end{cases}$
I_4	$\mu_{41}(t_4)=\begin{cases}1 & t_4<12.5\\ \frac{1}{2}\sin\left(\frac{t_4}{25}\pi\right)+\frac{1}{2} & 12.5\le t_4\le 37.5\\ 0 & t_4>37.5\end{cases}$	$\mu_{42}(t_4)=\begin{cases}0 & t_4<12.5\\ \frac{1}{2}\sin\left(2\pi-\frac{t_4}{25}\pi\right)+\frac{1}{2} & 12.5\le t_4\le 37.5\\ \frac{1}{2}\sin\left(\frac{t_4}{25}\pi-\pi\right)+\frac{1}{2} & 37.5\le t_4\le 62.5\\ 0 & t_4>62.5\end{cases}$	$\mu_{43}(t_4)=\begin{cases}0 & t_4<37.5\\ \frac{1}{2}\sin\left(3\pi-\frac{t_4}{25}\pi\right)+\frac{1}{2} & 37.5\le t_4\le 62.5\\ 1 & 62.5<t_4<75\\ \frac{1}{2}\sin\left(\frac{t_4}{50}\pi-\pi\right)+\frac{1}{2} & 75\le t_4\le 125\\ 0 & t_4>125\end{cases}$	$\mu_{44}(t_4)=\begin{cases}0 & t_4<75\\ \frac{1}{2}\sin\left(3\pi-\frac{t_4}{50}\pi\right)+\frac{1}{2} & 75\le t_4\le 125\\ 1 & t_4>125\end{cases}$
I_5	$\mu_{51}(t_5)=\begin{cases}1 & t_5<2.5\\ \frac{1}{2}\sin\left(\frac{t_5}{5}\pi\right)+\frac{1}{2} & 2.5\le t_5\le 7.5\\ 0 & t_5>7.5\end{cases}$	$\mu_{52}(t_5)=\begin{cases}0 & t_5<2.5\\ \frac{1}{2}\sin\left(2\pi-\frac{t_5}{5}\pi\right)+\frac{1}{2} & 2.5\le t_5\le 7.5\\ \frac{1}{2}\sin\left(\frac{t_5}{5}\pi-\pi\right)+\frac{1}{2} & 7.5\le t_5\le 12.5\\ 0 & t_5>12.5\end{cases}$	$\mu_{53}(t_5)=\begin{cases}0 & t_5<7.5\\ \frac{1}{2}\sin\left(3\pi-\frac{t_5}{5}\pi\right)+\frac{1}{2} & 7.5\le t_5\le 12.5\\ 1 & 12.5<t_5<15\\ \frac{1}{2}\sin\left(\frac{t_5}{10}\pi-\pi\right)+\frac{1}{2} & 15\le t_5\le 25\\ 0 & t_5>25\end{cases}$	$\mu_{54}(t_5)=\begin{cases}0 & t_5<15\\ \frac{1}{2}\sin\left(3\pi-\frac{t_5}{10}\pi\right)+\frac{1}{2} & 15\le t_5\le 25\\ 1 & t_5>25\end{cases}$
I_6	$\mu_{61}(t_6)=\begin{cases}1 & t_6<0.5\\ \frac{1}{2}\sin(t_6\pi)+\frac{1}{2} & 0.5\le t_6\le 1.5\\ 0 & t_6>1.5\end{cases}$	$\mu_{62}(t_6)=\begin{cases}0 & t_6<0.5\\ \frac{1}{2}\sin(2\pi-t_6\pi)+\frac{1}{2} & 0.5\le t_6\le 1.5\\ 1 & 1.5<t_6<3\\ \frac{1}{2}\sin\left(\frac{t_6-1}{4}\pi\right)+\frac{1}{2} & 3\le t_6\le 7\\ 0 & t_6>7\end{cases}$	$\mu_{63}(t_6)=\begin{cases}0 & t_6<3\\ \frac{1}{2}\sin\left(\frac{9-t_6}{4}\pi\right)+\frac{1}{2} & 3\le t_6\le 7\\ 1 & 7<t_6<7.5\\ \frac{1}{2}\sin\left(\frac{t_6}{5}\pi-\pi\right)+\frac{1}{2} & 7.5\le t_6\le 12.5\\ 0 & t_6>12.5\end{cases}$	$\mu_{64}(t_6)=\begin{cases}0 & t_6<7.5\\ \frac{1}{2}\sin\left(3\pi-\frac{t_6}{5}\pi\right)+\frac{1}{2} & 7.5\le t_6\le 12.5\\ 1 & t_6>12.5\end{cases}$

I_7	$\mu_{71}(t_7)=\begin{cases}1 & t_7<0.1\\ \frac{1}{2}\sin(5t_7\pi)+\frac{1}{2} & 0.1\le t_7\le 0.3\\ 0 & t_7>0.3\end{cases}$	$\mu_{72}(t_7)=\begin{cases}0 & t_7<0.1\\ \frac{1}{2}\sin(2\pi-5t_7\pi)+\frac{1}{2} & 0.1\le t_7\le 0.3\\ 1 & 0.3<t_7<0.35\\ \frac{1}{2}\sin\left(\frac{3}{2}\pi-\frac{0.65-t_7}{0.3}\pi\right)+\frac{1}{2} & 0.35\le t_7\le 0.65\\ 0 & t_7>0.65\end{cases}$	$\mu_{73}(t_7)=\begin{cases}0 & t_7<0.35\\ \frac{1}{2}\sin\left(\frac{3}{2}\pi-\frac{t_7-0.35}{0.3}\pi\right)+\frac{1}{2} & 0.35\le t_7\le 0.65\\ 1 & 0.65<t_7<0.75\\ \frac{1}{2}\sin(2t_7\pi-\pi)+\frac{1}{2} & 0.75\le t_7\le 1.25\\ 0 & t_7>1.25\end{cases}$	$\mu_{74}(t_7)=\begin{cases}0 & t_7<0.75\\ \frac{1}{2}\sin(3\pi-2t_7\pi)+\frac{1}{2} & 0.75\le t_7\le 1.25\\ 1 & t_7>1.25\end{cases}$
I_8	$\mu_{81}(t_8)=\begin{cases}1 & t_8<2.5\\ \frac{1}{2}\sin\left(\frac{t_8}{5}\pi\right)+\frac{1}{2} & 2.5\le t_8\le 7.5\\ 0 & t_8>7.5\end{cases}$	$\mu_{82}(t_8)=\begin{cases}0 & t_8<2.5\\ \frac{1}{2}\sin\left(2\pi-\frac{t_8}{5}\pi\right)+\frac{1}{2} & 2.5\le t_8\le 7.5\\ 1 & 7.5<t_8<10\\ \frac{1}{2}\sin\left(\frac{t_8}{10}\pi-\frac{1}{2}\pi\right)+\frac{1}{2} & 10\le t_8\le 20\\ 0 & t_8>20\end{cases}$	$\mu_{83}(t_8)=\begin{cases}0 & t_8<10\\ \frac{1}{2}\sin\left(\frac{1}{2}\pi-\frac{t_8}{10}\pi\right)+\frac{1}{2} & 10\le t_8\le 20\\ 1 & 20<t_8<22.5\\ \frac{1}{2}\sin\left(\frac{t_8}{15}\pi-\pi\right)+\frac{1}{2} & 22.5\le t_8\le 37.5\\ 0 & t_8>37.5\end{cases}$	$\mu_{84}(t_8)=\begin{cases}0 & t_8<22.5\\ \frac{1}{2}\sin\left(3\pi-\frac{t_8}{15}\pi\right)+\frac{1}{2} & 22.5\le t_8\le 37.5\\ 1 & t_8>37.5\end{cases}$

Table 4. The 1~9 scale method of factors comparison.

Scale value	Relative important explanation	Complementary value
1	Two factors contribute equally to the objective	1
3	One factor is slightly more important than the other	1/3
5	One factor is obviously more important than the other	1/5
7	One factor is strongly more important than the other	1/7
9	One factor is absolutely more important than the other	1/9
2, 4, 6, 8	Compromise value between two adjacent scales	1/2,1/4,1/6,1/8

For the specific solution process, please refer to references [40] and [41]. The subjective weight vector W^s is expressed as:

$$W=(w_1,w_2,\ldots,w_n) \tag{16}$$

Where w_i (i = 1, 2, …, n) is the weight value of the i-th evaluation index. Then, the consistency test of the initial weight of the evaluation index is carried out. The specific calculation steps refer to references [40] and [41].

Results and Discussion

Engineering Background

Longnan City in Gansu Province is one of the most developed and most densely distributed regions of debris flow in China, characterized by a wide distribution area, high frequency of occurrence, and serious harm, as shown in Fig. 4. Therefore, the Longnan region is taken as an example, and the risk assessment of debris flow gullies is carried out.

Data Acquisition

Ten representative debris flow gullies in the Longnan region are selected for the risk assessment. The measure values of the evaluation index of these 10 gullies are shown in Table 5.

Weighting Determination

Based on the 1~9 scale in Table 2, the triangular fuzzy judgment matrix is constructed, shown in Table 6. The weights of the evaluation index of debris flow are calculated.

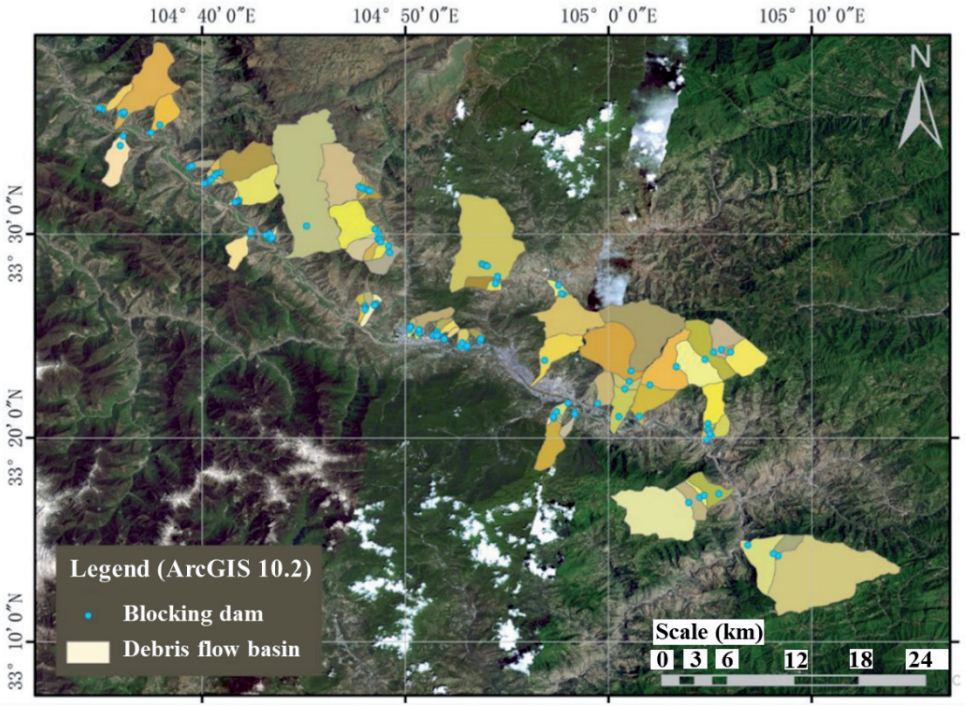

Fig. 4. Distribution map of debris flow gullies in the study region.

Risk Assessment of Debris Flow

The measure values of the evaluation index in Table 5 are substituted into Eq. (3) ~ Eq. (8). The synthetic attribute measure values for the risk of debris flow gullies are obtained, as shown in Table 7.

In the paper, the confidence level λ is taken as 0.65, and the ordered risk level set satisfies $C_1 > C_2 > ... > C_K$. Therefore, Eq. (12) is used to identify the risk level of debris flow. The risk level of 10 debris flow gullies can be obtained, as shown in Table 7.

Comparing the assessment results of the proposed method with those of the grey correlation model, it can be concluded that the assessment results of the other seven debris flow gullies are consistent except for Huoshao Gully, Guanjia Gully, and Ganjia Gully. We compared the assessment results of the proposed method in this paper with the actual field situations, and the results are as follows:

(1) The debris flow risk level of Huoshao Gully evaluated by the proposed method is grade III, while the risk level evaluated by the grey correlation is grade II. According to the actual field investigation, the gully bed is seriously scoured and undercut, and the bad geology is very developed. There are 33 landslides and collapses with an area of 3.15 km^2 and a solid material reserve of 8.3328×10^7 m^3. The average annual rainfall is 495.4 mm, and the rainfall from June to September accounts for

Table 5. Measure values of the evaluation index of 10 debris flow gullies.

Gully	I_1	I_2	I_3	I_4	I_6	I_8	I_{11}	I_{12}
Huoshao	2.95	1.98	12.1	0.648	1.35	63.5	17	48
Dongjiangshui	3.58	6.71	21.9	1.351	5.64	90.5	14	24
Niwan	7.2	10.3	17	1.23	5.34	63.5	27.8	23
Macao	19.7	13.5	18	0.983	4.3	39.7	83.33	22.8
Shiyanzi	8.6	13.7	32	1.586	6.1	330	26	26
Huama	10.3	17.8	28	1.08	5.4	330	31	20
Guanjia	23.7	35.01	22	2.201	10.2	70	115.39	21.6
Ganjia	38.4	43.3	23.9	1.135	12	78.6	134.13	9.5
Shimen	12.1	45.8	35	1.15	11.5	63.5	3.6	10
Beiyuhe	189.6	432	30	0.885	50	63.5	371.55	1.77

Table 6. Triangular fuzzy judgment matrix for index weights analysis.

Index	I_1	I_2	I_3	I_4	I_5	I_6	I_7	I_8
I_1	(1,1,1)	(2,3,4)	(2,3,4)	(2,2,3)	(2,2,3)	(1/3,1/2,1)	(1,2,3)	(1,1,1)
I_2	(1/4,1/3,1/2)	(1,1,1)	(1/2,1/2,1)	(1/3,1/2,1/2)	(1/3,1/3,1/2)	(1/5,1/4,1/3)	(1/3,1/3,1/2)	(1/4,1/3,1/3)
I_3	(1/3,1/2,1)	(2,3,3)	(2,3,4)	(2,3,3)	(1,2,3)	(1/4,1/3,1/3)	(1,1,1)	(1,1,2)
I_4	(1,2,3)	(3,4,5)	(3,3,4)	(2,3,3)	(2,3,3)	(1,1,1)	(3,3,4)	(2,2,3)
I_5	(1/4,1/3,1/2)	(1,2,2)	(1,1,1)	(1/3,1/2,1/2)	(1/2,1/2,1)	(1/4,1/3,1/3)	(1/4,1/3,1/2)	(1/3,1/3,1/2)
I_6	(1/3,1/2,1/2)	(2,2,3)	(2,2,3)	(1,1,1)	(1,1,1)	(1/3,1/3,1/2)	(1/3,1/3,1/2)	(1/2,1/2,1)
I_7	(1/3,1/2,1/2)	(2,3,3)	(1,2,2)	(1,1,1)	(1,1,1)	(1/3,1/3,1/2)	(1/3,1/2,1)	(1/2,1/2,1/2)
I_8	(1,1,1)	(3,3,4)	(2,2,3)	(1,2,2)	(2,2,2)	(1/3,1/2,1/2)	(1/2,1/2,1)	(1,1,1)
Weight	W = (0.175, 0.046, 0.058, 0.087, 0.089, 0.265, 0.143, 0.137) CI = 0.051<0.1, CR = 0.036<0.1, the judgment matrix satisfies the consistency test							

Table 7. Synthetic attribute measure matrix of debris flow gullies in the Longnan region.

Gully	Synthetic attribute measure (μ_k)				Risk level of this method	Grey correlation model
	I	II	III	IV		
Huoshao	0.048	0.272	0.586	0.137	III	II
Dongjiangshui	0.004	0.205	0.595	0.196	III	III
Niwan	0	0.196	0.695	0.109	III	III
Macao	0	0.439	0.334	0.227	III	III
Shiyanzi	0	0.155	0.369	0.476	IV	IV
Huama	0	0.173	0.341	0.486	IV	IV
Guanjia	0	0.035	0.583	0.382	IV	III
Ganjia	0	0.142	0.414	0.443	IV	III
Shimen	0.143	0.137	0.311	0.409	IV	IV
Beiyuhe	0.137	0	0.339	0.524	IV	IV

65.2%, and 3 to 7 debris flows occur per year during the rainy season. The measured maximum flow velocity on the surface of the debris flow was 7.5m/s, the maximum flow rate was 246 m^3/s, and the maximum volume of debris flow at one time was $52.4\times10^4 m^3$. The risk level of debris flow is very high, so the assessment result of this method is more in line with the actual situation.

(2) The risk level of Guanjia Gully evaluated by this method is grade IV, while the risk level evaluated by the grey correlation is grade III. According to the actual field investigation, there have been six major debris flows since 1950. Among them, the disaster on August 6, 1982, was the most serious, with a flow rate of $482 m^3/s$ and a duration of 30min. It caused 33 deaths and more than 100 injuries, destroyed 672 houses, and blocked the water flow of the Baishui River for 6 min. There is a large amount of residual slope deposits on the slope of Guanjia Gully. The loose solid mass reserves are rich, and the debris flow risk is very high. Therefore, the assessment result of this method is more in line with the actual situation.

(3) The risk level of Ganjia Gully evaluated by this method is grade IV, while the risk level evaluated by the grey correlation is grade III. According to the survey, there have been 10 large-scale debris flows since the last century, of which the flow rate was 641 m^3/s on August 3, 1984. Small-scale debris flows occur almost every year, sometimes up to more than 10 times, and the average erosion modulus in the gully is 35400 $kg/(km^2 \cdot a)$. Due to the large scale and strong activity of debris flows, the fan-shaped land develops rapidly, which causes the riverbed width to be less than 50 m and a large amount of sediment deposition. The riverbed of the Bailong River rises by 10 cm every year. Since the 1950s, the Ganjia Gully has blocked the Bailong River four times, each time lasting for 2~3 h and creating a backwater stretching for several kilometers, which flooded nearly a thousand mu of farmland and destroyed water

conservancy and transportation facilities. Therefore, the assessment result of this method is more in line with the actual situation.

In summary, the assessment results of the proposed method are more in line with the actual situation, which verifies the effectiveness and practicability of the proposed method. Meanwhile, the proposed method has the advantages of clear risk grading and strong adaptability.

Conclusions

(1) According to the statistical analysis of the risk assessment factors, combined with the field investigation in Longnan region, the maximum outflow volume at one time I_1, watershed area I_2, watershed incision density I_3, main gully length I_4, maximum relative height difference of the watershed I_6, maximum daily rainfall I_8, loose solid mass reserves I_{11}, longitudinal slope drop of the main gully I_{12} are selected to construct the evaluation index system of debris flow risk. The grade criteria of the debris flow evaluation index are proposed.

(2) A new method for comprehensive risk assessment of debris flow based on the fuzzy attribute interval measure model and TFT-AHP weighting method is proposed to predict the risk of debris flow. A triangular fuzzy number $[t_j^L, t_j^M, t_j^U]$ is used to quantify the value of the evaluation index, including the lower limit t_j^L, the most probable value t_j^M, and the upper limit t_j^U. The traditional single-index attribute measure functions are improved to characterize the nonlinear relationship between disaster occurrence and influencing factors. The multi-index measure function and attribute recognition analysis method based on a random combination of multi-index attribute measures are developed. The combination weighting method based on the triangular fuzzy theory and AHP is established.

(3) The proposed method is applied to assess the risk of ten debris flow gullies in the Longnan region. The assessment results are compared with the results obtained by the grey correlation model and the actual field investigation situations. It is found that the proposed method is more in line with the actual situations, more applicable, and clearer in distinguishing the risk level, which provides an effective way to accurately evaluate the risk of debris flow.

The evaluation index of debris flow in this paper does not consider the differences between regions, and the evaluation index system will be revised in the future by collecting the influencing factors of debris flow in the Longnan region. In addition, it is difficult to determine the values of the evaluation index. In the next step, the values of evaluation indices can be determined using satellite remote sensing data.

Acknowledgments

This work was supported by the National Natural Science Foundation of China (Grant No. 52408415), the Second Tibetan Plateau Scientific Expedition and Research Program (Grant No. 20190ZKK0902), the China Postdoctoral Science Foundation (2024M752751), the Natural Science Foundation of Chongqing (cstc2021jcyj-msxmX0133), the Science and Technology Research Program of Chongqing Municipal Education Commission (Grant No. KJQN202300714, Grant No. KJQN201901423, Grant No.KJQN202201426), the Major Science and Technology Special Project of Gansu Province (No. 23ZDFA009), the Key Scientific and Technological Project of Gansu Academy of Sciences (No.2023ZDYF-03).

Conflict of Interest

The authors declare no conflict of interest.

References

1. MA C., DENG J., WANG R. Analysis of the triggering conditions and erosion of a runoff-triggered debris flow in Miyun County, Beijing, China. Landslides, **15** (12), 2475, **2018**.
2. WANG B.L., LI Y., LIU D.C., LIU J.J. Debris flow density determined by grain composition. Landslides, **15** (6), 1205, **2018**.
3. TAKAHASHI T. Debris Flow: Mechanics, prediction and countermeasures. United Kingdom: Taylor & Francis Ltd, **2019**.
4. BERNARD M., GREGORETTI C. The use of rain gauge measurements and radar data for the model-based prediction of runoff-generated debris-flow occurrence in early warning systems. Water Resources Research, **57** (3), e2020WR027893, **2021**.
5. XU Q., DONG X.J., LI W.L. Integrated space-air-ground early detection, monitoring and warning system for potential catastrophic geohazards. Geomatics and Information Science of Wuhan University, **44** (07), 957, **2019**.
6. ZHAO Y., MENG X.M., QI T.J., CHEN G., LI Y.J., YUE D.X., QING F. Modeling the Spatial Distribution of Debris Flows and Analysis of the Controlling Factors: A Machine Learning Approach. Remote Sensing, **13** (23), 4813, **2021**.
7. LONG K., ZHANG S.J., WEI F.Q., HU K.H., ZHANG Q., LUO Y. A hydrology-process based method for correlating debris flow density to rainfall parameters and its application on debris flow prediction. Journal of Hydrology, **589**, 125124, **2020**.
8. RAJIB A., LIU Z., MERWADE V., TAVAKOLY A.A., FOLLUM M.L. Towards a large-scale locally relevant flood inundation modeling framework using SWAT and LISFLOOD-FP. Journal of Hydrology, **581**, 124406, **2020**.
9. ZHOU Y.Y., YUE D.X., LIANG G., LI S.Y., ZHAO Y., CHAO Z.Z., MENG X.M. Risk Assessment of Debris Flow in a Mountain-Basin Area, Western China. Remote Sensing, **14** (12), 2942, **2022**.

10. OUYANG C.J., WANG Z.W., AN H.C., LIU X.R., WANG D.P. An example of a hazard and risk assessment for debris flows-A case study of Niwan Gully, Wudu, China. Engineering Geology, **263**, 105351, **2019**.
11. CUI P., ZOU Q. Theory and method of risk assessment and risk management of debris flows and flash floods. Progress in Geography, **35** (2), 137, **2016**.
12. GU X.B., WU Q.H., ZHU Y.H. The experimental investigation on the propagation process of crack for brittle rock similar material. Geotechnical and Geological Engineering, **37** (6), 4731, **2019**.
13. CHEN S.Y., ZOU Q., WANG B., ZHOU W.T., YANG T., JIANG H., ZHOU B., YAO H.K. Disaster risk management of debris flow based on time-series contribution mechanism (CRMCD): Nonnegligible ecological vulnerable multi-ethnic communities. Ecological Indices, **157**, 111266, **2023**.
14. SUN Y.Q., GE Y.G., CHEN X.Z., ZENG L., TANG Q., LIANG X.Y., YANG L.B. Analysis of the trigger conditions and activity trend in debris flow along Sichuan-Tibet traffic corridor (Xinduqiao-Changdu section) under environmental changes. Bulletin of Engineering Geology and the Environment, **83**, 189, **2024**.
15. TANG Y., GUO Z., WU L., HONG B., FENG W., SU X., LI Z., ZHU Y. Assessing debris flow risk at a catch ment scale for an economic decision based on the LiDAR DEM and numerical simulation. Frontiers in Earth Science, **10**, 821735, **2022**.
16. HSU Y.C., LIU K.F. Combining TRIGRS and DEBRIS-2D Models for the Simulation of a Rainfall Infiltration Induced Shallow Landslide and Subsequent Debris Flow. Water, **11**, 890, **2019**.
17. KUANG C.P., WANG J.Y., LIU G.F., HAO W.H. Numerical Study on Debris Flow under Different Rainfall Intensities at Gangou in Hongse Village, Dujiangyan. Journal of Tongji University (Natural Science), **43** (7), 1012, **2015**.
18. HU X.D., ZHANG L., HU K.H., CUI L., WANG L., XIA Z.Y., HUANG Q.Z. Modelling the evolution of propagation and runout from a gravel–silty clay landslide to a debris flow in Shaziba, southwestern Hubei Province, China. Landslides, **19**, 2199, **2022**.
19. QIAO Z., SHEN W., BERTI M., LI T.L. An advanced SPH model for protective constructions of debris flows adopting the modified HBP constitutive law. Landslides, **20**, 2437, **2023**.
20. TAYYEBI S.M., PASTOR M., STICKLE M.M. Two-phase SPH numerical study of pore-water pressure effect on debris flows mobility: Yu Tung debris flow. Computers and Geotechnics, **132**, 103973, **2021**.
21. WANG T., YIN K., LI Y., CHEN L.X., XIAO C.G., ZHU H.M., Westen C. Physical vulnerability curve construction and quantitative risk assessment of a typhoon-triggered debris flow via numerical simulation: A case study of Zhejiang Province, SE China. Landslides, **21**, 1333, **2024**.
22. NOCENTINI M., TOFANI V., GIGLI G., FIDOLINI F., CASAGLI N. Modeling debris flows in volcanic terrains for hazard mapping: the case study of Ischia Island (Italy). Landslides, **12**, 831, **2015**.
23. CAO P., HOU S.S., CHEN L., FENG Z., WANG L.C., LI A., LIU J.Y. Risk assessment of mass debris flow based on numerical simulation: An example from the Malu River Basin in Min County. The Chinese Journal of Geological Hazard and Control, **32** (2), 100, **2021**.
24. ZHANG A.L., DAI Z.W., QIN W.B., FU X.L., GAO J.X., GUO L.J., LIU L., JIANG X.N., WANG H. Risk assessment of the Xigou debris flow in the Three Gorges Reservoir Area. Frontiers in Ecology and Evolution, **11**, 1264936, **2023**.
25. DING X.Y., HU W.J., LIU F., YANG X. Risk assessment of debris flow disaster in mountainous area of northern Yunnan province based on FLO-2D under the influence of extreme rainfall. Frontiers in Environmental Science, **11**, 1252206, **2023**.
26. HE Y.F., DING M.T., ZHENG H., GAO Z.M., HUANG T., DUAN Y., CUI X.J., LUO S.Y. Integrating development inhomogeneity into geological disasters risk assessment framework in mountainous areas: a case study in Lushan–Baoxing counties, Southwestern China. Natural Hazards, **117**, 3203, **2023**.
27. TAN C., MA D.H., CHEN J.P., ZHANG W., XU X.C. risk assessment of debris flow in Wudongde Reservoir Area Based on Analytic Hierarchy Process and Fuzzy Comprehensive Evaluation. IOP Conference Series: Earth and Environmental Science, **570** (4), 042053, **2020**.
28. SHEN S.W., XIE H.E., XU Y., ZHANG M., NIU X.B., LI G.L. Fuzzy comprehensive evaluation of debris flow in Matun village, Laomao Mountain area, Dalian city. Arabian Journal of Geosciences, **13**, 49, **2020**.
29. NIU Q.F., LU M., LI Y.F., FENG Z.B., GAO W.X., LU X.L. Hazard assessment of debris flow in Lanzhou City of Gansu Province based on methods of grey relation and rough dependence. The Chinese Journal of Geological Hazard and Control, **30** (5), 48, **2019**.
30. ZHANG X.J. GU X.B. The application of gray system-variable fuzzy sets coupling theory on the susceptibility assessment of debris flow hazards. Frontiers in Environmental Science, **11**, 1291454, **2023**.
31. LIU D.Y., CONG K., WEI J., ZHANG W., HOU Y.J., HE B. Hazardousness evaluation of debris flow in Beishan Mountain of Wudu District based on ideal point method. Journal of Geological Hazards and Environment Preservation, **29** (2), 7, **2018**. (in Chinese)
32. GU X.B., MA Y., WU Q.H., JI X.J., BAI H. The risk assessment of landslide hazards in Shiwangmiao based on intuitionistic fuzzy sets-Topsis model. Natural Hazards, **9**, 283, **2021**.
33. LI Y.C., CHEN J.P., LI Z.H., HAN X.D., ZHAI S.J., LI Y.C., ZHANG Y.W. A case study of risk assessment of debris flow and hazard range prediction based on a neural network algorithm and finite volume shallow water flow model. Environmental Earth Sciences, **80**, 275, **2021**.
34. LI L., NI B., QIANG Y., ZHANG S., ZHAO D., ZHOU L. Risk assessment of debris flow disaster based on the cloud model-Probability fusion method. PLoS ONE, **18** (2), e0281039, **2023**.
35. XIAO Q., WANG S., HE N., GURKALO F. Risk Zoning Method of Potential Sudden Debris Flow Based on Deep Neural Network. Water, **16**, 518, **2024**.
36. CHOI G.M., LEE I.W., YUNE C.Y. Risk Assessment of Debris Flow at Regional Scale considering Catchment Area in Chuncheon, Korea. KSCE Journal of Civil Engineering, **25**, 1176, **2021**.
37. CHEN M., LUO Y., TANG C., LI N. Quantitative assessment of expected direct economic losses of buildings for debris flows in multiple rainfall intensity scenarios in Yangling Gully, Southwest China. Natural Hazards, **120** (3), 2993, **2023**.
38. LI Y., ZOU Q., HAO J., SU L. Risk Assessment of Debris Flows Along the Karakoram Highway (Kashgar-Khunjerab Section) in the Context of Climate Change. International Journal of Disaster Risk Science, **14** (4), 586, **2023**.

39. SUN Y., GE Y., CHEN X., ZENG L., LIANG X. Risk assessment of debris flow along the northern line of the Sichuan-Tibet highway. Geomatics and Natural Hazards and Risk, **14** (1), 2195531, **2023**.
40. WANG S., DING H., HUANG F., WEI Q., LI T., WEN T. Ideal point interval recognition model for dynamic risk assessment of water inrush in karst tunnel and its application. Polish Journal of Environmental Studies, **33** (2), 1, **2024**.
41. WANG S., LI L.P., CHENG S. Risk assessment of collapse in mountain tunnels and software development. Arabian Journal of Geosciences, **13**, 1196, **2020**.